VI. DISCUSSION

Figure 4 shows the reduced partial $M1$ mean life plotted with respect to mass number. The single-particle estimate of Moszkowski is shown as a horizontal line. In this very small sample there appear to be two groups, one about 20 times the single-particle estimate. Preliminary results on slightly heavier nuclei show some cases that fall between the two groups. The group of longer lifetime have the same reduced lifetimes as the group of L-forbidden transitions measured by DeWaard and Gerholm.[17]

In general the reduced partial $M1$ mean lives fall in the same region as among the heavy elements, and are somewhat longer than those found in the light elements.[18]

ACKNOWLEDGMENTS

We are indebted to A. Vandergust for construction and maintenance of much of the equipment, and to J. Wallace and the Van de Graaff group for operation of the electrostatic accelerator. Dr. J. Monahan made several statistical analyses of our data and helped us program them for the IBM-704 computer. Dr. E. N. Shipley helped in taking some of the data and coded the computer program to fit the tail of the time spectra by least squares.

[17] H. DeWaard and T. R. Gerholm, Nuclear Phys. **1**, 281 (1956).

[18] D. H. Wilkinson, Phil. Mag. **1**, 1031 (1956); *Proceedings of the Rehovoth Conference on Nuclear Structure*, edited by H. J. Lipkin (North-Holland Publishing Company, Amsterdam, 1958), p. 175; *Nuclear Spectroscopy*, edited by Fay Ajzenberg-Selove (Academic Press, Inc., New York, 1960), Part B, p. 852.

PHYSICAL REVIEW VOLUME 121, NUMBER 5 MARCH 1, 1961

Radiochemical Study of the Ranges in Metallic Uranium of the Fragments from Thermal Neutron Fission*

JAMES B. NIDAY
Lawrence Radiation Laboratory, University of California, Livermore, California
(Received September 23, 1960)

The mean ranges in uranium of 28 fission products have been determined by radiochemical measurement of the fraction escaping from the surface. Several factors affecting the precision and accuracy of the method are discussed. A semiempirical equation was developed which gave an excellent correlation between the ranges of fragments from a specific mass chain and their average initial velocity. The average total kinetic energy of the fragment pairs is about 30 Mev less for the products of symmetrical fission than is expected from comparison with the asymmetrical products. The low momenta of the symmetrical fragments are not readily explained by particle emission unless the concept of isotropic neutron evaporation is abandoned. The results may be interpreted by assuming that the symmetrical and asymmetrical products result from two modes of fission which involve different critical shapes of the fissioning nucleus, and that the choice between modes is dependent on the closing of the 50-proton shell in the heavy fragment. The 10% decrease in range observed for two shielded nuclides is also examined in some detail.

I. INTRODUCTION

MANY studies have been made of the ionization produced by fragments from various types of fission and a few studies of the ranges of various fragments in light mass absorbers. Previous work on the kinetic energies of fission fragment recoils was summarized by Walton in 1957.[1]

Most of the previous radiochemical work has involved considerable experimental difficulty in the handling of many samples collected in very thin absorbers. In 1955, a preliminary survey of the ranges of some of the fragments formed in the fission of uranium by high-energy particles was begun by a different technique which gives the mean range of a specific mass chain in metallic uranium. This method is based on radiochemical determination of the fraction of the fission fragments escaping from the surface of a "thick" fission source of known area.[2] These exploratory measurements did not readily lend themselves to interpretation, and it was decided to initiate a calibration program during which the reproducibility of this method could be studied. Since range measurements on fission produced by high-energy particles are affected by center-of-mass motion and by anisotropic angular distribution of the fragments, it was felt that the method should give results reliable to about $\pm 1\%$ to permit adequate interpretation.

Measurement of the ranges of fragments from thermal neutron fission of U^{235} offered a convenient means of evaluating other experimental variables, and these

* This work was performed under auspices of the U. S. Atomic Energy Commission.

[1] G. N. Walton, *Progress in Nuclear Physics* (Butterworths—Springer, London, 1957), Vol. 6, pp. 192–232.

[2] This "integral range method" has been used by Batzel, Sugarman, and others in studies of high-energy recoil fragments. See, e.g., R. E. Batzel and G. T. Seaborg, Phys. Rev. **82**, 607 (1951); and N. T. Porile and N. Sugarman, Phys. Rev. **107**, 1410 (1957).

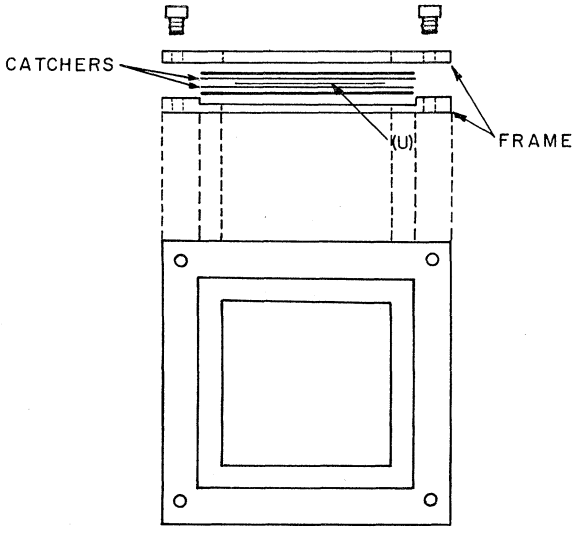

FIG. 1. Schematic diagram of foil assembly.

ranges are of considerable theoretical and practical interest in themselves. A fairly detailed picture of the relation between the mean ranges of various mass chains and their mass number was sought for two reasons. Average "smooth curve" values were needed for comparison with the ranges of specific fragments (i.e., the "shielded nuclides") formed directly in fission. Also, it seemed desirable to establish whether or not the range vs mass curve for U^{235} would show a significant decrease near symmetrical mass division as found by Katcoff *et al.*[3] in the case of Pu^{239} fission. Kinetic energy studies of U^{235} and Pu^{239} fission[4,5] have also indicated, although with considerable uncertainty, that the average total kinetic energy decreased for mass ratios below about 1.25. This point is of some importance in connection with various theories of fission; see, e.g., Fong.[6]

II. GENERAL EXPERIMENTAL PROCEDURE

The source foils were taken from 0.001-inch rolled stock of normal or enriched uranium by cutting carefully with a scalpel around the edge of a 4-cm×4-cm hardened steel block. The first few runs were made using foils cleaned in dilute nitric acid and in acetone, but most of the foils were electropolished to a smooth, bright surface, washed in acetone, and air-dried before weighing. Most of the catcher foils were 0.001-inch aluminum and were washed to remove surface impurities. The oxide-free uranium foil was then centered between the two $2\frac{1}{4}$-in.×$2\frac{1}{4}$-in. catcher foils. This sandwich was backed up by 0.005-inch aluminum foils on each side for rigidity, and the whole clamped tightly in a "picture frame" aluminum clamp for irradiation (Fig. 1). The rate of oxidation of uranium in this arrangement was quite slow compared with that of exposed metal. Fourteen of the irradiations reported here were made in the Water Boiler thermal column and thirteen in the higher and more uniform flux of the new Livermore Pool Type Reactor (LPTR).

After an amount of irradiation and cooling appropriate to the nuclides being studied, the two catcher foils and the uranium foil were dissolved separately. The solvents varied from 6*N* HCl (usually containing a few drops of H_2O_2 or HNO_3) to concentrated HNO_3 (containing a little Cl^-, F^-, or Hg_2^{++} ion to catalyze the dissolution of aluminum). A known amount of the appropriate inactive isotopic carrier was then added to these solutions, or to aliquot portions of them. Each solution was then subjected to the usual radiochemical operations of forcing "exchange" between the carrier and the various possible chemical species of the fission product, removal of undesired elements, and precipitation of the carrier in a form suitable for weighing, mounting, and counting.

Details of the radiochemical purification procedures used are outlined in Appendix II. Most of these were in current use in this Laboratory,[7] and were well established. Occasionally, additional steps were taken to ensure very high purity or to separate from other carriers added simultaneously. For some of the elements studied, special precautions were necessary in the initial operations to prevent loss of some of the fission product activity before exchange with the isotopic carrier was complete. For example, tellurium is readily lost as H_2Te when highly electropositive metals such as aluminum and uranium are being dissolved, unless the solvent is a powerful oxidizing agent. Consistent results were obtained, however, when the foils were dissolved slowly in concentrated HNO_3 containing a few drops of HCl and the resulting solutions fumed down to produce Te^{VI} before making the initial reduction to Te metal.

No procedure for ruthenium was available in the literature which would ensure solution of the metal and give exchange between carrier and fission product ruthenium before some losses occurred. After numerous trials, the following procedure was devised which gave more consistent results: The foils were dissolved in aqua regia, the entire solution plus carrier was made basic, oxidized carefully to Ru^{VI} and Ru^{VII}, divided into aliquots and reduced before preparing for the usual purification by distillation of RuO_4. The operations up to this point were carried out in a quantitative manner.

After purification, the final precipitates were dried and transferred to aluminum dishes, weighed on a semimicrobalance for determination of the relative chemical yields, and mounted on heavy aluminum

[3] S. Katcoff, J. A. Miskel, and C. W. Stanley, Phys. Rev. **74**, 631 (1948).
[4] W. E. Stein, Phys. Rev. **108**, 94 (1957).
[5] D. C. Brunton and G. C. Hanna, Can. J. Research **A28**, 190 (1950); D. C. Brunton and W. B. Thompson, Can. J. Research **28**, 498 (1950).
[6] P. Fong, Ph.D. dissertation, University of Chicago, 1953 (unpublished); see also Phys. Rev. **102**, 434 (1956).
[7] Several of these procedures were described in the University of California Radiation Laboratory Report UCRL-4377, August 10, 1954 (unpublished).

plates for counting. The mounting plates used after the first four early experiments had been machined to give a tolerance of about 0.001 inch in the distance between the sample and the counter. This distance varied from about $\frac{1}{4}$ in. to $2\frac{5}{8}$ in., but was usually about $\frac{7}{8}$ in. The relative activities of most of the nuclides were determined by counting gamma and bremsstrahlung radiations by means of NaI(Tl) scintillation crystals. The crystals were shielded from beta particles by a heavy beryllium absorber and pulses of less than 15 kev were not counted. These counters were quite stable and were used wherever possible in order to avoid the uncertainties involved in counting beta particles from samples of varying thickness. Small corrections were applied to the gamma-counting data for Mo^{99}, mounted as $PbMoO_4$, because of absorption by the lead of low-energy gamma radiation. A proportional counter was used for counting the beta radiations from Sr^{89}, Sr^{90}, Ag^{111}, $Pd^{109,112}$ (first run) directly and from Rb^{86}, Y^{93}, Ru^{106}, and Ce^{144} through appropriate absorbers. (Y^{93}, Ru^{106}, and Ce^{144} were also determined by gamma counting.) In the case of Sr^{89}, $Pd^{109,112}$, and Ce^{144}, it was possible to make approximate corrections for the relative variation of self-scattering and absorption of the beta radiations with the mass of the sample.

After sufficient counting data were accumulated, the decay curves were analyzed to obtain the relative activity of a given nuclide in each sample at a fixed time. In nearly all cases the analysis was made with the aid of an IBM 650 computer using a code which gives a least-squares fit to an exponential decay curve. This method of counting and analysis proved to be more reliable and more convenient than rotation counting for obtaining relative counting rates at a specific time. The relative activities were, of course, corrected for chemical yield of the carrier and size of aliquot taken.

It is easily shown (see Appendix IA) that one-fourth of the fragments produced in a layer whose depth is equal to the range will escape from the surface of the source foil. (Corrections necessary for nonuniform production through the foil are discussed in Sec. IIIG and Appendix IB.) The range of a given nuclide is then simply four times the ratio of its activity in one catcher to the total activity in all three foils multiplied by the thickness of the uranium foil in mg/cm^2.

III. EVALUATION OF SOURCES OF ERROR

A. Determinate Errors of the Radiochemical Procedure

The primary sources of error considered in this section are pipetting, weighing and mounting of samples, counting statistics, radioactive purity, resolution of decay curves, and self-scattering and absorption of beta radiation in the samples. Some problems usually associated with radiochemical work, e.g., determination of counting efficiencies for the radiations and standardization of carrier solutions, did not appear in this study because only relative activities were needed.

The final samples were weighed by a technique for which a standard deviation of about ± 0.01 mg has been established and most of the samples used weighed from 10 to 25 mg. The errors from statistical variations in counting rate were kept low by preparation of highly active samples wherever feasible. The chemical procedures used have been shown to give adequate radioactive purity and the radioactive decay of the samples was carefully monitored.

The range calculation also involves the thickness and area of the uranium foils. Any errors in weighing these foils should be completely negligible and their areas are believed to be consistent to about $\pm 0.1\%$.

In nearly all the runs the catcher foils were analyzed in duplicate and the uranium foil in quadruplicate. The agreement between these replicates was used to calculate a standard deviation in the activity ratio which included the effect of random variations in the weighing and mounting of samples, pipetting technique, and analysis of the radioactive decay. In addition, for each experiment a separate estimate was made of the effect of possible errors in the factory calibration of any pipets and volumetric flasks used and in the area of the uranium foil. These errors were combined to give an estimated standard deviation for the individual range determination.

The errors associated with self-scattering and absorption of beta radiations in the samples are extremely difficult to evaluate and may result in larger deviations than those indicated by the statistical agreement of replicate samples. All determinations based on beta counting have been so labeled.

B. Activation of Impurities

Neutron activation of impurities present in the catcher foils could result in erroneous range values for certain nuclides or at least interfere with the resolution of the decay curves for isotopic or chemically similar species. The amount of each element which could be tolerated as an impurity was calculated from the estimated ranges and from published values for isotopic abundances, neutron capture and fission cross sections, and fission yields. Most of the possibilities were easily eliminated by spectroscopic analysis of a sample catcher foil. In many cases blanks were determined by analysis of an extra piece of foil placed behind a catcher during the irradiation. In general, no corrections for impurities were necessary.

C. Surface Condition of the Uranium Foils

The cleaning procedures employed were described above. The necessity of removing the heavy coating of oxide frequently found on uranium was confirmed by one experiment in which the apparent range of Mo^{99} determined for an oxide-covered foil was at least 3%

lower than in other runs. There is some indication that somewhat higher range values were obtained with electropolished foils than in the early runs with acid-cleaned foils, but the introduction of other improvements in technique at about the same time forestalled any definite conclusions.

D. Uniformity of Source Foils and Neutron Flux

No critical study was made of the uniformity in thickness of the uranium foils. One set of nine foils cut from a single piece of uranium had a consistent pattern of weights (taken after electropolishing) which implied a maximum thickness variation of about one percent across the 4-cm width of one foil. The flux patterns in the thermal columns were mapped roughly by activation of small copper disks, and a maximum fluctuation of about $\pm 3.5\%$ across a foil diagonal was found. The most unfavorable combination of such uniform fluctuations across the foil would not affect the measured ranges appreciably.

In the few experiments made at the LPTR with enriched uranium, the activity of the catcher foils differed by about 2 to 4%. Copper neutron detectors centered on the outside of the catchers showed a similar effect. These variations were attributed to flux depletion (Sec. IIIG) and orientation towards the reactor core and they were averaged out in the calculation of ranges and standard deviations for these runs.

E. Thermal Diffusion of Fission Fragments

The possibility of errors resulting from diffusion of fission products in the metallic foils was considered to be negligible. The most obvious possibility, thermal diffusion of the short-lived rare-gas precursors of Sr^{89}, Cs^{137}, and Ba^{140}, should be quite negligible at ordinary temperatures.[8] The foil assembly was such as to provide good thermal contact with the environment, but, as a precaution, the temperature rise of an enriched-uranium foil was measured during a run by means of a thermocouple. Under conditions estimated to produce 1.4 watts in the foil, the maximum temperature rise of only 1°C was the same as that expected for the ambient air.

F. Nuclear Scattering Effect

The theoretical equations of Bohr and others[9–11] for range and straggling of fission fragments in the nuclear stopping region near the end of their range do not cover the present case of stopping by atoms heavier than the fragments. The last part of the path will be dominated by diffusion effects[9,12] with large deflections and large energy losses occurring in the collisions. The "mean range" measured in these experiments is, of course, an arithmetical average of the distance between the origin and the final resting place of the fragment. Large angular deflections could cause more fragments to scatter out of the uranium foil than would scatter back from light mass catchers and the calculated mean range would then be too high. Cloud chamber photographs of fission fragment tracks sometimes show significant bending,[13] and it was suggested[14] that this effect might be a serious source of error in the uranium range measurements.

Three additional runs were carried out using normal uranium surrounded by lead catcher foils to check this effect. Lead was chosen as the nearest to uranium in mass of the convenient heavy elements. The ranges obtained in this way were lower than the aluminum catcher results by $\sim 5\%$ for light fragments (Sr,Zr) and $\sim 3\%$ for heavy fragments (Ba,Ce). This is about the effect to be expected for hard-sphere collisions near the end of the range (see Sec. VA).

G. Corrections for the Enriched Uranium Experiments

In order to compare the ranges measured in highly enriched uranium with those determined in ordinary uranium, the former values must be corrected for the difference in masses and for the depression of neutron flux by U^{235}. If one assumes that the two materials have the same number of atoms per cm^3, and will stop any given fragment in the same number of collisions, then the equivalent range in normal uranium (in mg/cm^2) is higher by the ratio of the average atomic weights.

The flux depletion inside highly enriched uranium foils is quite large and a nonlinear function of depth. Correction factors for the resulting apparent increase in range were calculated for each experiment (see Appendix IB) and varied from about 0.085% to 1.46%. When these factors were combined with the opposite correction for the U^{238}/U^{235} mass ratio, the net correction for range measurements made in the enriched foils was usually very small.

IV. RESULTS

The range values obtained are given in Table I. Standard deviations were assigned to the results of individual runs by the somewhat arbitrary procedure described in Sec. IIIA. These estimates were used as weighting factors in obtaining the final averages.

The initial objective of studying the reproducibility of the experimental method has been fairly well satisfied. Two or three determinations appear to be sufficient for about one percent reliability in the range of a nuclide when such radiochemical criteria as reasonable counting

[8] K. E. Zimen and L. Dahl, Z. Naturforsch. **12a**, 167 (1957).
[9] N. Bohr, Kgl. Danske Videnskab. Selskab, Mat.-fys. Medd. **18**, No. 8 (1948).
[10] J. Lindhard and M. Scharff, Kgl. Danske Videnskab. Selskab, Mat.-fys. Medd. **27**, No. 15 (1953).
[11] R. B. Leachman and H. Atterling, Arkiv Fysik **13**, 101 (1958).
[12] K. O. Nielsen, in *Electromagnetically Enriched Isotopes and Mass Spectrometry*, edited by M. L. Smith (Butterworth and Company, London, 1956), pp. 68–81.
[13] J. K. Bøggild, O. H. Arrøe, and T. Sigurgeirsson, Phys. Rev. **71**, 281 (1947).
[14] J. M. Alexander (private communication).

TABLE I. Fission fragment ranges in uranium.

Element	Mass	Counting method	Al catchers: No. of determinations	Al catchers: Weighted average (mg/cm²)	Al catchers: Std deviation	Pb catchers: No. of determinations	Pb catchers: Weighted average (mg/cm²)	Pb catchers: Std deviation
As	77	γ	1	12.9	±0.2			
Rb[a]	86	β	1	10.5	±0.1			
Sr	89	β	6	11.55	±0.05			
Sr	90	β	1	11.9	±0.3			
Sr, Y	91	γ	3	11.54	±0.07	2	11.05	±0.05
Y	93	$\gamma-\beta$	1	11.35	±0.08			
Zr	95	γ	2	11.36	±0.04	2	10.80	±0.05
Zr	97	γ	2	11.36	±0.03	2	10.84	±0.05
Mo	99	γ	7	11.17	±0.06	1	11.3	±0.1
Ru	103	γ	2	11.28	±0.05			
Ru	106	$\gamma-\beta$	2	10.9	±0.1			
Pd	109	$\beta-\gamma$	2	10.09	±0.09			
Ag	111	β	2	9.74	±0.08			
Pd	112	$\beta-\gamma$	2	9.61	±0.06			
Cd	115	γ	3	9.52	±0.05			
Sn	125	$\beta-\gamma$	3	9.09	±0.09			
Sb, Te	127	γ	3	9.58	±0.04			
Te	129^m	γ	2	9.75	±0.03			
Te	132	γ	3	9.63	±0.03			
Cs[a]	136	γ	2	8.36	±0.04			
Cs	137	γ	2	9.18	±0.04			
Ba	140	γ	4	8.74	±0.05	3	8.50	±0.03
Ce	141	γ	3	8.56	±0.02	3	8.27	±0.05
Ce	143	γ	4[b]	8.42	±0.04	2	8.16	
Ce	144	$\beta-\gamma$	2	8.34	±0.10	1	8.15	
Nd	147	γ	1	8.07	±0.05			
Sm	153	γ	1	7.43	±0.07			
Eu	156	γ	1	7.1	±0.1			

[a] Shielded isotope.
[b] All based on unpolished foils.

rate, radioactive purity, exchange, and known counting corrections and half-lives are satisfactorily met. No runs meeting these criteria were excluded from the table.

The weighted average of seven determinations of Mo^{99} appears low in relation to the nearby mass chains but the spread of values obtained suggests further study for possible radiochemical difficulties, especially since most of the values were lower than that for the single run with a lead catcher. There is also some indication of possible surface effects in that a number of other measurements in the five early runs made with acid-cleaned rather than electropolished uranium foils were 1 to 3% lower than in the later runs. In the absence of more information on the statistical agreement to be expected, however, they were included in the final averages.

The experiments with lead catchers show that the actual "mean range" in uranium (see Sec. IIIF and VA) varies from 5 to 3% less (see Fig. 2) than the values given for aluminum catchers. However, the latter values will be equally useful for most of the correlations which are made below. It should be noted that they are also of practical use in any calculations of the escape of fragments from a uranium surface which is not in contact with material of high atomic weight.

The plot of ranges versus mass numbers shown in Fig. 2 definitely indicates a considerable lowering in total kinetic energy release for U^{235} in the region of nearly symmetrical fission between mass numbers 104 and 130. One can draw in a definite peak in the range curve at a mass ratio of about 1.25. The general shape of the curve bears a relation to the fission yield vs mass number curve[15] for U^{235} similar to that which can be seen for the data of Katcoff *et al.* on the ranges of plutonium fission fragments in air[3] and the corresponding fission yield curve[15] for Pu^{239}.

The ionization chamber studies of Brunton and Hanna[5] and the direct velocity measurements of Stein[4] also indicated a maximum total kinetic energy release in U^{235} fission at a mass ratio of about 1.25. A simple normalization of the present measurements to their data indicates, however, that their kinetic energy values for mass ratios less than 1.2 were not low enough. This would not be surprising in view of the small number of coincidences which they measured in this region of low fission yield, especially in the velocity studies.

The range of the shielded nuclide Cs^{136} was found to be almost 10% lower than would be predicted for this mass number on the basis of a smooth curve. There

[15] E. P. Steinberg and M. S. Freedman, *Radiochemical Studies: The Fission Products* (McGraw-Hill Book Company, Inc., New York, 1951), Paper No. 219, National Nuclear Energy Series, Plutonium Project Record, Div. IV, Vol. 9.

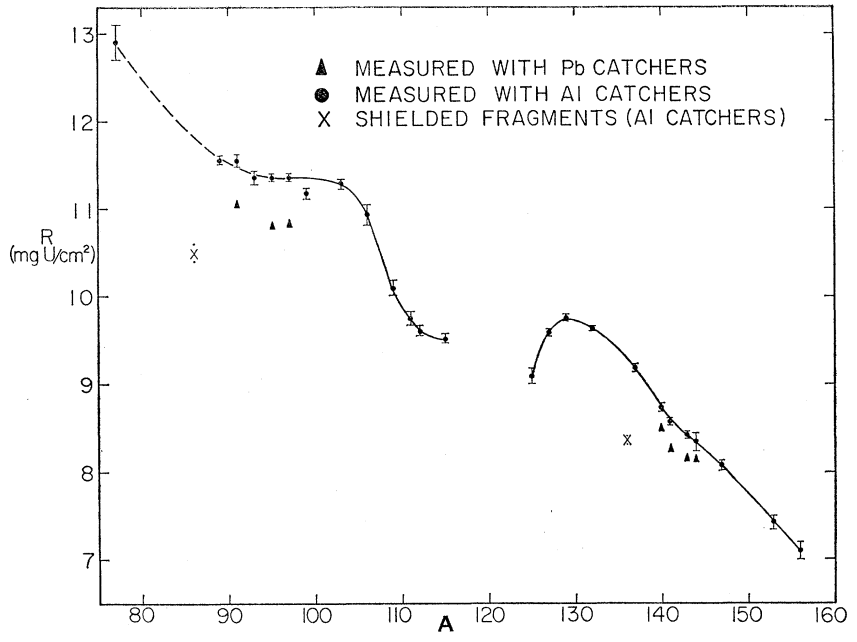

FIG. 2. Measured ranges.

seems to be no reason to question the validity of this number since the radiochemical procedure has been used many times with exceptionally good results and also because the range of Cs^{137} was determined simultaneously. For similar reasons, the single determination from one of the same runs of the range of the other shielded nuclide, Rb^{86}, can also be reported with reasonable confidence. The range deficiency for Rb^{86} appears to be slightly greater but the exact location of the smooth curve value in this region is less certain as yet. The low ranges for the symmetrical fission region and for the two shielded nuclides will be discussed below.

V. DISCUSSION

A. Correlation of Range with Charge and Velocity

Theoretical analysis of the stopping of fission fragments in matter is difficult because of the continual capture and loss of electrons along the path and the importance of elastic collisions between screened nuclei in the low-energy region after the ionic charge has been neutralized. The subject was treated extensively by Bohr[9] and his approach has been applied to data on ionic charge and energy loss of fission fragments in gases by Lassen.[16] Bohr divides his stopping power equation into two parts representing the major effect of electronic stopping and the additional effect of collisions without ionization when the velocity, V, has become less than $V_0=e^2/\hbar$, the "velocity" of an electron in the hydrogen atom. As mentioned previously the second part is applicable only when the stopping atoms are lighter than the fragment. However, near the end of the range in a very heavy stopping material such as uranium there will be rapid loss of energy and large angle scattering as in the diffusion of neutrons.[12] The vector sum of these small parts of the path should, on the average, make only a minor perturbation in the total range.

With this in mind, it is interesting to correlate the present range measurements with published velocity data using only the part of Bohr's equation for the stopping power due to electronic collisions in heavy materials [see Eq. (3.5.7) in reference 9]. This equation is derived from the Fermi-Thomas statistical model of the atom and, although approximate, is supposed to be valid for comparison with alpha particle ranges and, therefore, should be valid for comparisons between fission fragments.

$$-(\Delta E/\Delta R)_{\text{ion}}=NB_e n_e(3H^{-\frac{1}{3}}+H^{-1}), \qquad (1)$$

where

$$B_e=2\pi e^4 Z_1{}^{*2}/(mV^2), \quad n_e=2Z_2{}^{\frac{1}{3}}V/V_0, \quad H=2Z_1{}^*V_0/V.$$

N represents the number of atoms per unit range, e and m are the electronic mass and charge, and Z_1 and Z_2 are the nuclear charges of the fragment and the stopping atoms. The effective average charge is considered to be a function of the velocity, $Z_1{}^*=KV/V_0$, where $K=k\eta_s$, and η_s is the effective quantum number of the outer electrons of the ion. This number was estimated to be about $Z_1{}^{\frac{1}{3}}$ for the heavy fission fragments slowing down in gases and somewhat less for light fragments because of a proposed limitation[17] that Z^* must be less than $Z/2$. These considerations (with $k=1$) appeared to fit the data of Lassen fairly well.[17,18] The effective charge of the

[16] N. O. Lassen, Kgl. Danske Videnskab. Selskab, Mat.-fys. Medd. **25**, No. 11 (1949).

[17] N. Bohr and J. Lindhard, Kgl. Danske Videnskab. Selskab, Mat.-fys. Medd. **28**, No. 7 (1954).

[18] N. O. Lassen, *Proceedings of the International Conference on Peaceful Uses of Atomic Energy, Geneva, 1955* (United Nations, New York, 1956), Vol. 2, p. 214.

fragments in solids is much more difficult to evaluate, but it is expected to be higher because of the much shorter time between collisions[17] and/or because of polarization of the environment.[19] A qualitative estimate of $Z^*=1.5\eta_s V/V_0$ was made by Bohr and Lindhard.[17]

It should be noted that the data on the average charge of fragments emerging into vacuum[18,20] from a uranium source require K to be about $1.4Z_1^{\frac{1}{3}}$ for the heavy fragments but require $K=Z_1^{\frac{1}{3}}$ or else $K=1.4Z_1^{0.235}$ for the light fragments.

Using Eq. (1) and $dE=AVdV$, where A is the mass of the fragment observed, and integrating between the initial velocity and the velocity at which ionization becomes negligible, V_0, to get the range equation, one finds

$$R=\frac{AV}{CNZ_2^{\frac{1}{3}}f(Z_1)V}\int_{V_i}^{V_0}dV=\frac{A(V_i-V_0)}{CNZ_2^{\frac{1}{3}}f(Z_1)}, \qquad (2)$$

where $f(Z_1)=(K+4.7622K^{5/3})$. Substituting suitable constants such that A is in units of mass number, V in units of 10^8 cm/sec, and R in mg/cm^2 of uranium, one obtains

$$R_U=\frac{A(V_i-V_0)}{2.411(K+4.7622K^{5/3})}. \qquad (3)$$

As a first approximation, ranges in uranium were calculated from this formula using the relatively simple relation $K=Z_1^{\frac{1}{3}}$. The nuclear charge values were taken from Nethaway's empirical table[21] of the most probable charges (Z_p) for each mass chain, or were calculated[21] from the equal charge displacement hypothesis.[22] The initial velocities, V_i, were obtained from Stein's plot of total kinetic energy versus mass ratio (see Fig. 6 in reference 4) by taking into account his assumption that 1.25 neutrons were lost isotropically from each fragment. The ranges calculated for the peak yield light masses were about 4% higher than the measurements made with aluminum catchers, and those for the heavy masses were less than 1% higher. This is a remarkably good agreement considering the number of uncertainties involved in the derivation of the equation, in the rather crude estimation of Z^*, in the lower limit used in the integration (V_0), and in the contribution of nuclear scattering to the total range. Although the agreement may be somewhat fortuitous, a modified form of the equation will be very useful for comparative purposes (Sec. VB and VC). Several comments should be made first on the effective charge function and on scattering.

It is apparent that as an ion loses most of its charge, the effective quantum number η_s must decrease toward unity for the outermost electrons. The agreement between the calculated and measured values can be improved by arbitrary choice of an average η_s less than $Z_1^{\frac{1}{3}}$, k greater than one, and different limits of integration for dV. However, the range data and the published average charges of fragments emerging from solids into a vacuum[18,20] mentioned above do not appear to fit the same function of Z_p. If $K=1.5Z_1^{\frac{1}{3}}$ is substituted in Eq. (3), following the suggestion of Bohr and Lindhard[17] mentioned above, the ranges calculated are about a factor of two lower than those observed. It should be noted also that Leachman and Schmitt[23] obtained three data points for the initial slowing of median-heavy fragments in gold foils which will fit Eq. (2) approximately if K is assumed equal to $Z_1^{\frac{1}{3}}$ as in the above calculations.

Bohr's limitation that Z^* should always be less than $Z/2$, which would cause even higher calculated ranges for masses less than 106, does not seem to apply, except perhaps for the single high point at As[77]. Also, the stopping power found for the other light fragments is about 30% greater than for the heavy, in contrast to Lassen's data for argon gas[16] but in agreement with Northrop and Brolley's data[24] for UO_2.

The slightly lower ranges obtained by using lead rather than aluminum to catch the escaping fragments imply that significant scattering occurs along the path of the fragments in heavy materials. This should occur largely for the fully screened atoms near the end of their range, since Rutherford scattering is predominantly at small angles, and the difference in the two measurements should provide some measure of the volume through which the diffusion occurs (see also Sec. IIIF). The scattering in the transition region for velocities near V_0 is difficult to treat theoretically. According to Bohr, isotropic scattering should begin when the "collision diameter" b $[b=2Z_1Z_2e^2/(\mu V^2)]$ is greater than the "screening radius" a $[a=a_0/(Z_1^{\frac{2}{3}}+Z_2^{\frac{2}{3}})^{\frac{1}{2}}]$, which occurs for the average fragment at about $\frac{2}{3}V_0$. (μ is the reduced mass of the system and a_0 is the "first Bohr radius" of the hydrogen atom.)

By equating b and a, one can calculate for any fragment a critical energy, E_c, corresponding to a critical velocity, V_c, below which the scattering may be assumed to be of the hard-sphere type. Nielsen has estimated[12] the penetration of low-energy particles (45 kev) into materials of greater atomic weight by calculating the Fermi age, τ, in analogy with neutron diffusion calculations. Although the average number of collisions required to stop fission fragments of energy E_c in uranium is too small for true diffusion behavior, the use of the appropriate values of τ in the range calculation (Appendix IA) will account for the differences between ranges measured with lead and aluminum catchers. This

[19] J. Neufeld and W. S. Snyder, Phys. Rev. **107**, 96 (1957).
[20] B. L. Cohen, A. F. Cohen, and C. D. Coley, Phys. Rev. **104**, 1046 (1956).
[21] D. R. Nethaway (private communication), and Ph.D. dissertation, Washington University, St. Louis, Missouri, 1959 (unpublished).
[22] L. E. Glendenin, C. D. Coryell, and R. R. Edwards, Paper No. 52, reference 15.
[23] R. B. Leachman and H. W. Schmitt, Phys. Rev. **96**, 1366 (1954).
[24] J. A. Northrop and J. E. Brolley, Jr., Bull. Am. Phys. Soc. **28**, 19 (1953).

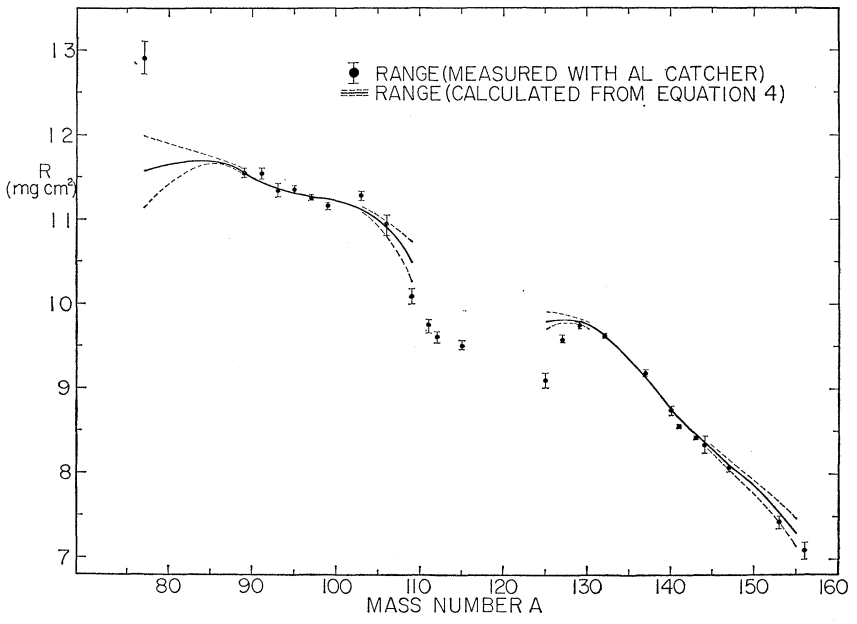

FIG. 3. Measured ranges vs Eq. (4). The line was calculated from the semiempirical range equation [Eq. (4)] by using initial velocities from reference 4, Z_p calculated from the equal-charge-displacement hypothesis, and the effective charge function $K=1.077Z_p^{\frac{1}{3}}$.

appears to support a rough model of the slowing down process in which it is assumed that scattering occurs predominantly near the end of the path and is nearly isotropic and, therefore, that the path length calculated for ionizing collisions can be a fairly good measure of the effective mean range in heavy materials.

Determination of better parameters for range and velocity correlations with this model would seem to require more information on the variation of the average effective charge and on the scattering behavior of the fragments. Nevertheless, it is possible to adjust these parameters arbitrarily to obtain a very useful semiempirical equation. If the integration [of Eq. (2)] with respect to velocity is carried down to V_c, rather than to V_0, the shape of the calculated range curve corresponds to the measured values much more closely:

$$R=\frac{A(V_i-V_c)}{2.411(K+4.762K^{5/3})}.$$

The measured ranges can now be reproduced quite well by appropriate adjustment of the parameter k in the effective charge function, $K=kZ_p^{\frac{1}{3}}$. The choice of $k=1.077$ gives calculated ranges in excellent agreement with the aluminum catcher measurements (see Fig. 3) for fragments of high fission yield (i.e., well-known velocities). The average deviation for the light fragments (about -0.4% for masses 89 to 97) is now within the precision of the range and velocity data. The large deviation at mass 77 and the questionable value for mass 99 have already been discussed. The actual "mean range in uranium," as measured with lead catchers, may be reproduced satisfactorily by substituting $K=1.1Z_p^{\frac{1}{3}}$ in Eq. (4).

B. Symmetrical Fission

The striking dip in the range vs mass number curve in the region of symmetrical fission (Fig. 2) can now be examined in greater detail. The initial velocity of each primary fragment, and then the corresponding fragment energy (E_f), may be calculated from the range measured with aluminum catchers by using Eq. (4) and the relation $K=1.077Z_p^{\frac{1}{3}}$. The total kinetic energy release (E_T) is now readily obtained from conservation of momentum if the average initial mass (M) of the observed mass chain (A) is known. Such calculations are based on the apparently reasonable assumption[25] that the prompt neutrons are evaporated from the fully-accelerated fragment in such a way that the fragment velocity in the laboratory system is unchanged, on the average.

The total kinetic energies calculated for mass chains between 103 and 132 by assuming that the observed fragment lost 1.25 neutrons on the average ($M-A=\nu_x=\bar{\nu}/2$) are plotted versus mass ratio in Fig. 4 along with a reproduction of Stein's curve[4] which has been adjusted slightly in the region of high mass ratios by using data obtained in this work.

A distinction has been made in plotting points calculated from the ranges of fragments whose masses are greater (M_H) or less (M_L) than 118, in order to simplify discussion of the limitations on ν_x. If, for example, $\nu_L>1.25$ the corresponding E_T is greater but M_H/M_L is less and the plotted point (✕) must be moved in the "eleven-o'clock direction" from the location shown. On the other hand, if $\nu_H>1.25$ both E_T and the mass ratio are larger and the corresponding point (●) must move toward "one-o'clock." As plotted, the E_T values obtained from heavy and light masses form self-consistent

[25] J. Terrell, Phys. Rev. **113**, 527 (1959).

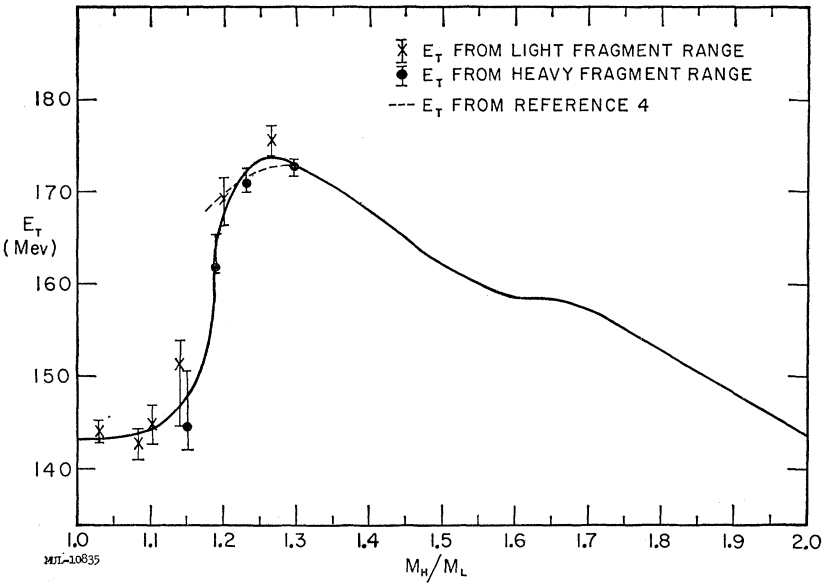

FIG. 4. Average total kinetic energy vs mass ratio. Energies were calculated from velocities by assuming that the observed fragment lost 1.25 prompt neutrons. Velocities were calculated from ranges by means of Eq. (4). The errors shown include a postulated variation in average nuclear charge near $Z=50$ (see text). Above $M_H/M_L=1.25$, the solid line is based primarily on the data of reference 4 but has been adjusted slightly at high mass ratios by comparison with the results obtained in this work.

sets with an apparent discrepancy between them which might imply a somewhat different distribution of neutron numbers (at least $\nu_L<1$). This discrepancy is completely removed, however, if one assumes that a strong tendency to form a closed shell of fifty protons increases the average charge of the primary fragments in any mass chain for which the predicted distribution[21,22] around Z_p contains a significant fraction of elements 48 and 49. The positive and negative limits of error assigned to E_T (estimated from the uncertainties in range and charge) for $A=106$, 109, 125, and 127 have been adjusted accordingly. It should be noted that these errors are no longer independent and that the location of the best line through the present data is not very sensitive to this correction.[26]

From Fig. 4 it is apparent that the drop in total kinetic energy release for mass ratios below 1.2 is much sharper than would have been anticipated from Stein's data. Fong has made calculations[6] based on the liquid-drop model of the nucleus of the Coulomb energy release vs mass ratio by assuming a particular nuclear configuration during fission. It seems reasonable to use these Coulomb energies as a standard for comparison because they are nearly equal to Stein's E_T at the mass ratio for peak kinetic energy (1.25 ± 0.01). On this basis E_T is about 31 Mev less than expected for mass ratios below 1.1.

In seeking an explanation of this kinetic energy deficiency for nearly symmetrical fission, one may first examine hypotheses involving loss of additional neutrons or other particles. If there is an unusual amount of distortion in the compound nucleus at the moment of scission, this extra energy may be expended by evaporation of additional neutrons from one or both of the fragments, or an alpha particle may split off.[27,28] The most critical test of these hypotheses is found at $M_H/M_L\sim1.15$ where the deficiency in E_T is still 25–30 Mev. The data in this region are somewhat uncertain for a definitive momentum balance, but they do imply that not more than four mass units could have been lost, if the assigned errors are realistic. An inspection of the fission yield vs mass curve,[15,29] which is changing rapidly in the mass region of interest here, shows that the fission yields of corresponding heavy and light fragments cannot be matched if more than about three mass units have been lost.

With this limitation on the masses, the low kinetic energies cannot be accounted for by the loss of small particles unless the concept of isotropic evaporation of neutrons from fully accelerated fragments[25] is abandoned, at least for this mass region. If there is excessive distortion, the separated fragments may be more likely to contract in such a way as to concentrate their energy[27] and eject high-energy neutrons in the forward direction. It is possible to account for the missing energy and also balance the momenta in the entire region below mass ratio 1.25 (peak E_T) if one makes the rather extreme assumption that one high-energy neutron was ejected from each fragment.

In this connection it should be observed that the sharp decrease in E_T is closely related to mass ratios for

[26] If the data shown in Fig. 4 are recalculated using the recently published distribution of ν_L and ν_H [V. F. Apalin, U. P. Dobrinin, V. P. Zaharova, I. E. Kutikov, and L. A. Mikhaylan, Atomnaya Energ. 8, 15 (1960)], the steep portion of the curve shifts to slightly lower mass ratios and the sets of points calculated from light and heavy mass chains diverge considerably. Use of the proposed shift in $\bar{Z}$ brings most of these points into agreement but leaves a discrepancy of ~2 standard deviations at the peak E_T.

[27] D. L. Hill and J. A. Wheeler, Phys. Rev. **89**, 1102 (1953).

[28] The "long-range alphas" are emitted in a direction nearly perpendicular to the fragments with a most probable energy of about 15 Mev and in an abundance roughly equal to the total fission yield in the mass region under discussion.

[29] S. Katcoff, Nucleonics **16**, No. 4, 78 (1958).

which the equal charge displacement hypothesis gives most probable charges of 48.5 to 49 for the heavy fragment. If one postulates a strong tendency for the heavy fragment to be built up around a 50-proton core, it seems reasonable to suppose that those critical shapes which tend to result in an incomplete proton shell would involve excessive distortion. It was noted above that the total kinetic energies calculated from the ranges of masses 106, 109, 125, and 127 are in better agreement if it is assumed that the closed proton shell has a significant effect on the average nuclear charge. The data available on E_T vs mass ratio for several other fission processes, $Pu^{239}(n,f)$,[3–5] $U^{233}(n,f)$,[4,5] $Th^{229}(n,f)$,[30] Cf^{252} (spontaneous fission),[31,32] also seem to be consistent with the idea that the decrease in energy for the symmetrical fission mode is related to the closing of the 50-proton shell. It is also of interest that there are other indications from fission yield data[33–35] that symmetrical and asymmetrical fission may involve somewhat different processes, perhaps with different configurations for the fissioning nucleus.

Many of the above considerations about possible neutron losses depend on the validity of the ranges for the two mass chains 109 and 125. Further work on these and other nearby chains should be carried out, along with a consideration of the fact that they are both isomeric states.

In connection with the two-mode-of-fission hypothesis and the effect of the 50-proton shell, it should be of interest to study the range behavior of symmetrical and asymmetrical fission products from compound nuclei with varying amounts of excitation energy.

C. Shielded Nuclides

The low ranges of Cs^{136} and Rb^{86} were also evaluated with the aid of the stopping power equations. Of course, the range will be somewhat less than expected for the normal chain, even for the same initial velocity, primarily because of the increase in $Z^*(Z_{\text{shielded}}>Z_p)$.

About one-fourth of the 10% deficiency in range for Cs^{136} can be accounted for by the increased stopping power for the actual nuclear charge of 55 as compared with the Z_p of 52.5 for the mass chain 136. The energy calculated for the Cs^{136} fragment, using Eq. (4) and $Z_1=55$, is 61.6 Mev, and E_T is about 148.6 Mev, if an average loss of 1.25 neutrons is assumed. This is still about 20 Mev less than Stein's velocity measurements[4] gave for this mass ratio.

For such atypical mass splittings (representing about 10^{-3} and 10^{-5}, respectively, of the total yield for these mass chains), some of the potential energy of fission normally available as kinetic energy may be released in other ways. A thermodynamic analysis was made, from the total masses of the various products, of the difference in the amount of energy available as kinetic energy for the two processes: (a) the "normal" splitting for mass 136, with $Z_1=Z_p$ and the usual average number of prompt neutrons emitted ($\bar{\nu}=2.5$); and (b) the shielded mass splitting, with $Z_1=55$ and various numbers of neutrons (ν) evaporated from the two fragments. Each process must follow the equation

$$M(_{92}{}^{236})^*=M(_{Z_1}{}^{136})+M(_{92-Z_1}{}^{100-\nu})+\nu M(_0{}^1)+\nu\bar{E}_n+E_\gamma+E_T, \quad (5)$$

in which E_γ represents the average total prompt gamma emission, and $\bar{E}_n$ represents the average c.m. (evaporation) energy of the neutrons. The values used for $M(_Z{}^A)$, the ground-state masses of the fragments after prompt neutron emission, were based on Levy's empirical mass equation.[36]

The evaporation energy of the neutrons was estimated from Terrell's relation,[25] $\bar{E}_n=0.621(\nu+1)^{\frac{1}{2}}$, but E_γ was assumed to be the same for the two processes. By subtraction, a series of values was obtained for the *difference* in E_T between processes (a) and (b) as a function of ν for process (b). Next, E_T for process (b) was calculated from the observed E_{136} (61.6 Mev) for each of various possible numbers of neutrons evaporated from the Cs fragment itself. These total energies were subtracted from Stein's[4] E_T of 168.3 Mev for process (a).

Comparison of these two sets of energy differences then showed that ν for process (b) must be $4(\pm1)$ and the number from the Cs fragment alone must be between 0 and 3.

In the region of Rb^{86} the position of the range curve for typical fragments and the behavior of the effective average charge are somewhat uncertain. However, similar calculations gave essentially identical results for the permissible variation in prompt neutron losses.

The low ranges of the shielded nuclides may thus be attributed to the combined effect of higher distortion energy with lower Coulomb repulsion, and higher total beta-decay energy (because the partners of the shielded fragments are very far from stability), in addition to the effect of the nuclear charge on the stopping power. Further work is planned on the ranges of shielded nuclides.

ACKNOWLEDGMENTS

The author wishes to express his appreciation for helpful discussions with his co-workers Dr. P. C. Stevenson, Dr. H. G. Hicks, Dr. H. B. Levy, and Dr. D. R.

[30] A. Smith, P. Fields, A. Friedman, and R. Sjoblom, Phys. Rev. **111**, 1633 (1958).
[31] J. C. D. Milton and J. S. Fraser, Phys. Rev. **111**, 877 (1958); W. E. Stein and S. L. Whetstone, Jr., Phys. Rev. **110**, 476 (1958).
[32] The distribution of fission yields for Cf^{252} is such that the sharp drop in E_T, if any, should be confined to about two mass splittings and difficult to detect. See W. E. Nervik, P. C. Stevenson, H. G. Hicks, H. B. Levy, J. B. Niday, and J. C. Armstrong, Bull. Am. Phys. Soc. **4**, 372 (1959); and (to be published).
[33] A. Turkevich and J. B. Niday, Phys. Rev. **84**, 52 (1951).
[34] G. P. Ford, Phys. Rev. **118**, 1261 (1960).
[35] H. B. Levy, H. G. Hicks, P. C. Stevenson, J. B. Niday, and J. C. Armstrong, Bull. Am. Phys. Soc. **5**, 347 (1960).
[36] H. B. Levy, Phys. Rev. **106**, 1265 (1957). J. Riddell, Chalk River Laboratory Report CRP-654, 1956 (unpublished).

Nethaway, and also with Dr. J. Alexander, Dr. N. Sugarman, Dr. A. Turkevich, and Dr. J. Wheeler. He is especially indebted to Nancy Lee, Joyce Gross, and Dolores Razavi for their assistance in counting the samples.

APPENDIX I

A. Escape of Fission Fragments from the Uranium Foil

The following is generalized from the derivation of Walton and Croall.[37] The probability that a given fission fragment originating in the layer dx will move in the angle increment $d\theta$ from the foil normal and $d\phi$ in the plane of the surface (see Fig. 5) is $\sin\theta d\theta d\phi/4\pi$ for isotropic emission. The number of fragments formed in a layer of unit area and dx cm thick is $I_{(x)}dx$, and those of range R directed between $\theta=0$ and $\theta=\cos^{-1}(x/R)$ will emerge from the surface.

For the general case, the number of fragments escaping from unit area of the surface into the catcher is

$$N_C=\frac{1}{4\pi}\int_{x=0}^{R}\int_{\theta=0}^{\arccos(x/R)}\int_{\phi=0}^{2\pi} I_{(x)}J(\theta,\phi)\sin\theta dx d\theta d\phi.$$

For fission induced by high-energy particles, any preferred orientation of the fragment direction in the laboratory system is included in the function $J(\theta,\phi)$, and any center-of-mass motion along the foil normal may be analyzed by appropriate changes in the limits of integration (with respect to x) for the "forward" and "backward" directions. The total number of fragments formed in a foil of thickness t is

$$N_T=\int_{x=0}^{t} I_{(x)}dx.$$

For the case of thermal neutron fission with constant flux throughout the foil, $J(\theta,\phi)=1$, the function $I_{(x)}$ is constant, and

$$N_C=\tfrac{1}{2}I\int_{x=0}^{R}\int_{\theta=0}^{\arccos(x/R)}\sin\theta dx d\theta$$
$$=\tfrac{1}{2}I\int_{x=0}^{R}\left(1-\frac{x}{R}\right)dx=\tfrac{1}{4}IR,$$

and

$$N_T=I\int_{x=0}^{t}dx=It.$$

Then the range in uranium is calculated from the activity ratio

$$A_C/A_T=N_C/N_T=R/4t.$$

[37] G. N. Walton and I. F. Croall, J. Inorg. & Nuclear Chem. **1**, 149 (1955).

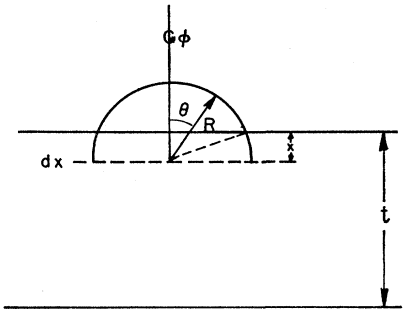

FIG. 5. Diagram for calculation of fractional escape.

B. Effect of the Flux Depletion in Enriched Uranium

When highly enriched uranium is irradiated with thermal neutrons the flux is significantly higher near the surface than in the interior of the foils and the function $I_{(x)}$ must be included in the integration with respect to x of the equations given above for N_C and N_T. This was done by first calculating the fraction of the surface flux ($I_{(x)}$ varies directly as the flux) which will reach the layer dx from each side of the foil for various values of x. After compiling a table of these fractions, the equations for N_C and N_T given above were integrated numerically by Simpson's rule for various total thicknesses of uranium.

The relative flux in the layer dx is

$$\int_0^1 \exp\left(-\frac{x\sigma N}{\cos w}\right)d\cos w + \int_0^1 \exp\left(-\frac{(t-x)\sigma N}{\cos w}\right)d\cos w,$$

where N is the number of atoms per cm^3, σ is the average total absorption cross section of the material used, and $x/\cos w$ is the path length in uranium of a neutron entering the foil at an angle w from the perpendicular. Numerical evaluation of these integrals proved to be awkward because of the sensitivity to small values of $\cos w$, so the following transformation was made.[38] Substituting $c=x\sigma N$ and $\cos w=1/Z$ and then integrating by parts, this becomes

$$\int_0^\infty \frac{e^{-cZ}}{Z^2}dZ=e^{-c}-c\int_1^\infty \frac{e^{-cZ}}{Z}dZ.$$

With another substitution of $y=cZ$, this becomes

$$e^{-c}-c\int_c^\infty \frac{e^{-y}}{y}dy=e^{-c}-cE_1(c).$$

[38] This transformation was kindly pointed out by R. E. Shafer.

The expansion of the $E_1(c)$ function,

$$E_1(c)=-\gamma-\ln c-\sum_{n=1}^{\infty}\frac{(-1)^n c^n}{n\times n!},$$

converges well enough for small values of c. Then the relative flux *from one surface* at the layer dx is

$$e^{-c}+c\left(0.577216+\ln c-c+\frac{c^2}{4}-\frac{c^3}{18}+\frac{c^7}{96}\cdots\right).$$

Detailed numerical integrations of N_C and N_T were then made for selected high, medium, and low values of R at three different total foil thicknesses using a table of 75 values of relative flux vs c. Then the ratio of N_C to that which would be expected if the corresponding N_T represented a uniform average flux through the foil is very nearly the ratio of the measured range to that which would be obtained if there were no flux depletion. These corrections were plotted and interpolated values were used to correct the various ranges measured in enriched uranium.

APPENDIX II. OUTLINE OF CHEMICAL PROCEDURES

The anion columns referred to in several of the following procedures consisted of 6-mm×10-cm beds of Dowex 1×8, 50–100 mesh resin equilibrated with the first reagent to be used. The "mixed hydroxide" scavenges used in several procedures were made by adding a mixture of iron, zirconium, tellurium, and lanthanum carriers before making the solution basic. The final precipitates were washed thoroughly with the appropriate acids, water, or other solvents before drying at 110–125°C.

Arsenic was precipitated as As_2S_3 from a 9*M* HCl solution containing iodide ion, and dissolved in conc. HCl containing chlorate ion. The solution was adjusted to 9*M* HCl and passed through a column of anion resin. The eluate was treated with conc. HNO_3 and $HClO_4$ and fumed to a small volume of $HClO_4$. The arsenic was extracted into benzene from 3*M* HCl containing HI and back-extracted into water. The sulfide was precipitated again from 9*M* HCl, dissolved, and fumed to a small volume of $HClO_4$. Finally, arsenic was reduced to the metal with chromous chloride.

Strontium was separated along with barium in most cases by means of anion columns, ammoniacal scavenges, and/or precipitation of strontium and barium as nitrates or carbonates. Three or more barium chromate precipitations were made at *p*H 5. Strontium was recovered as the carbonate, passed through an anion column in 6–9*M* HCl solution, scavenged with mixed hydroxides, and finally precipitated as $SrCO_3$.

Zirconium was separated as the hydroxide, dissolved in 4*M* HNO_3, extracted into benzene which was 0.1*M* in TTA, washed four times with 4*M* HNO_3 (containing nitrite the first two times), and back-extracted into 9*M* HCl which was 2*M* in HSO_4^-. After this solution was diluted with an equal volume of water, zirconium was recovered as the phosphate, and ignited to ZrP_2O_7.

Molybdenum was adsorbed on anion resin from a 4–6*M* HCl solution. The column was washed with 0.1*M* HCl and 3*M* NH_4OH and the molybdenum eluted with 4*M* HNO_3. The solution was scavenged with mixed hydroxides by adding enough conc. NH_4OH to reach *p*H 10. After a preformed scavenge with iron and lanthanum hydroxides the supernate was acidified with acetic acid and $PbMoO_4$ was precipitated.

Ruthenium was determined successfully by the following procedure: The metal foils were dissolved in 6*M* HCl which was about 1*M* in HNO_3 and contained the Ru^{III} carrier. After some digestion the solution was made 1.5–2*M* in OH^- (conc. K_2CO_3 solution was used for the uranium solution), enough KIO_4 was added to produce a red color (Ru^{VI}), and the solution was heated and allowed to cool. At room temperature just enough 5% NaOCl was added to give a greenish tint (Ru^{VII}) and the solution was digested cold. After division into aliquots of roughly equal size, more base, some solid $Na_2S_2O_4$, and a few glass beads were added. The resulting precipitate was coagulated by gentle boiling, separated, and dissolved in 6*N* HCl containing a few drops of conc. HNO_3. Conc. H_2SO_4 was then added and the solution boiled to copious fumes. This solution was diluted to 5–6*N* in H_2SO_4, solid $NaBiO_3$ added, and RuO_4 distilled into cold 12*M* NaOH. The trap solution was diluted to 2–3*N* in NaOH and ruthenium reduced with ethyl alcohol. The precipitated oxides were dissolved in the minimum volume of 6*N* HCl and Ru^0 precipitated with magnesium metal.

Palladium was separated as PdI_2, dissolved in conc. HCl containing a drop of HNO_3, and the nitrate ion reduced with formic acid. The palladium was then adsorbed on Dowex-1 resin, washed with 0.1*M* HCl and with 4*M* HNO_3, and eluted with 3*M* NH_4OH. The eluate was scavenged with mixed hydroxides and with zirconium phosphate. The final precipitation of palladium was made with dimethyl glyoxime.

Silver was separated initially as AgCl from a 4*M* HNO_3 solution or as Ag_2S from a 6*N* HCl solution followed by precipitation of AgCl. The precipitate was dissolved in NH_4OH, scavenged with $Fe(OH)_3$ after adding a trace of iodide ion, and silver sulfide was precipitated in the presence of EDTA. Further hydroxide scavenges and two precipitations of AgCNS were made before the final reduction to Ag^0 with ascorbic acid.

Cadmium was precipitated as the hydroxide in the presence of molybdenum and antimony carriers, dissolved in 2*M* HCl and the solution scavenged with antimony and palladium sulfides. The cadmium was then adsorbed on Dowex 1 resin, washed with 0.1*M* HCl and eluted with 1.5*M* H_2SO_4. The eluate was scavenged with mixed hydroxides in the presence of excess NH_4OH and a final precipitation of CdS was made from slightly acid solution.

Tin was separated from foils dissolved in a strongly oxidizing acid medium and was precipitated initially as the hydroxide or the sulfide. In the first experiment hydroxide, iodide, and sulfide (in the presence of fluoride) scavenges were made. Tin was then precipitated as the sulfide, dissolved in a polysulfide solution, and passed through an anion column. Tin was recovered as the hydroxide and ignited to SnO_2. In the second experiment the tin was extracted into hexone from 6*M* HCl containing holdback carriers of antimony, molybdenum, and tellurium and back-extracted into 1*M* HCl containing fluoride. Scavenges with arsenic sulfide and molybdenum α-benzoin oxime were alternated with precipitations of SnS_2. This precipitate was dissolved in saturated sodium sulfide. The tin was adsorbed on Dowex 1 resin from dilute sulfide solution and then eluted with saturated Na_2S before the final precipitation.

Antimony was separated from foils dissolved in two different ways. In the first experiment they were dissolved in conc. HNO_3 containing a little hydrochloric acid and antimony was separated initially as the sulfide. In the second run the foils were dissolved in KOH solution containing H_2O_2 which was then acidified for an initial separation of metallic antimony (by reduction with hydroxylamine and chromous chloride) before the sulfide step. The rest of the procedure involved precipitations of the metal and the sulfide in the presence of various holdback carriers, and scavengings with tellurium and arsenic sulfides. The antimony was adsorbed on anion resin from strong HCl, washed with 1*M* HCl and 9*M* H_2SO_4, and eluted with boiling 2*M* NaOH solution. The final precipitation to the metal from 1*M* HCl was made with chromous chloride.

Tellurium determinations were made from foils dissolved slowly in nitric acid (containing a little chloride or other catalyst for the aluminum foils). Tellurium was reduced from Te^{VI} to Te^{IV} by heating with hydrochloric acid. Two reductions of tellurium to the metal with stannous chloride were alternated with caustic hydroxide scavenges and a final reduction was made with gaseous SO_2.

Cesium and rubidium were separated and purified together by a procedure whose essentials have been published.[39] This procedure used several hydroxide scavenges, made first with ammonia and then with sodium hydroxide, and a sulfide scavenge. The cesium and rubidium were precipitated as the perchlorates, dissolved in water and separated on a Duolite *C*-3 cation column with 0.3*N* HCl, and finally precipitated as the perchlorates.

When cesium alone was determined, separation from rubidium was unnecessary and a shorter procedure was used. Cesium was precipitated initially as cesium silicotungstate which was then dissolved in a minimum volume of 2*M* LiOH. The cesium was absorbed on a short column of Dowex-50 cation resin, eluted with 6*N* HCl, and the eluate passed through an anion column. After scavenging with hydroxide (using sodium hydroxide), the final precipitate of cesium perchlorate was prepared and washed thoroughly with ethyl acetate.

Barium was separated from strontium (see above) as the chromate, precipitated as the chloride three times from an ether-HCl mixture, scavenged in the same manner as strontium and finally recovered as barium chromate.

Cerium was separated initially as the hydroxide after passing through an anion column and carried through two cycles of the customary zirconium iodate scavengings and ceric iodate precipitations and passed through an anion column in conc. HCl. The final precipitate of cerium oxalate was ignited to ceric oxide.

The rare earths and yttrium were precipitated as the fluorides in the presence of dichromate and numerous holdback carriers, redissolved in the presence of boric acid, scavenged with barium sulfate, and recovered as the hydroxides. They were then dissolved in conc. HCl, passed through an anion column, and scavenged with zirconium phosphate from 4*N* HCl. A second hydroxide precipitate was dissolved in 6 drops of conc. HNO_3, diluted to 30 ml, and adsorbed on Dowex-50 resin. The elements were separated by gradient elution with ammonium lactate, precipitated with oxalic acid and ignited to the oxides.

[39] J. B. Niday, Phys. Rev. **98**, 42 (1955).